Applied Science and Engineering Progress, Vol. 19 No. 4, 2026, 8193

Research Article

The Effect of $CaCl_2$ Cross-Binding Agent Concentration on Alginate-Carboxymethyl Cellulose-Oil Palm Empty Fruit Bunches Gel Granules as a Methylene Blue Adsorbent

Firda Dimawarnita*, Yora Faramitha, Fayyadh Altamis Erwinsyah, Donny Nugroho Kalbuadi, Indah Puspita Sari and Didiek Hadjar Goenadi
Indonesian Oil Palm Research Institute, Bogor, Indonesia

Tiasuri Pangastuti
Department of Chemical Analysis, Vocational School, IPB University, Bogor, Indonesia

Pijar Religia
International Center for Biotechnology, Osaka University, Osaka, Japan

* Corresponding author. E-mail: firda.dimawarnita@gmail.com DOI: 10.14416/j.asep.2026.06.005
Received: 31 January 2026; Revised: 24 March 2026; Accepted: 27 May 2026; Published online: 9 June 2026

Abstract
Water pollution caused by synthetic dye waste, such as methylene blue, poses a serious environmental problem due to its resistance to natural degradation. This issue can be addressed by utilizing carboxymethyl cellulose (CMC) derived from oil palm empty fruit bunches (OPEFB), which not only helps reduce palm oil industry waste but also produces value-added materials for environmental applications. This study aimed to investigate the effect of varying concentrations of calcium chloride ($CaCl_2$) as a crosslinking agent on the synthesis of alginate–CMC gel beads derived from OPEFB, used as adsorbents for methylene blue wastewater. The study was conducted in three stages: synthesis, characterization, and application, using $CaCl_2$ concentrations of 3%, 4%, 5%, 6%, and 7%. The observed parameters included swelling ratio, functional group interactions (FTIR), surface morphology (SEM), and adsorption capacity for methylene blue. The results indicated that the optimal $CaCl_2$ concentration was 3%, achieving the highest swelling ratio of 65.35% and a maximum adsorption capacity of 3.59 mg/g. Characterization results showed that increasing the $CaCl_2$ concentration led to the formation of a denser gel structure with lower swelling capacity, as supported by SEM images, which revealed more compact surfaces at a 7% concentration. FTIR spectra confirmed the formation of ionic crosslinking between the polymer carboxylate groups and Ca^{2+} ions, as indicated by characteristic band shifts at 1614 cm^{-1}. The findings emphasize that controlling the $CaCl_2$ concentration is crucial for producing gel beads with optimal physical properties and enhanced adsorption performance.

Keywords: Adsorbent, Calcium chloride, Gel beads, Methylene blue, Oil palm empty fruit bunches

1 Introduction

The palm oil industry is a strategic sector of the Indonesian economy. According to data from the Oil Palm Plantation Fund Management Agency, Indonesia's oil palm production reached approximately 42 million tons, with a total land area exceeding 14 million hectares in 2021 [1]. According to the 2023 Indonesian Palm Oil Statistics Publication, palm oil production has reached 50.07 million tons with a land area of 16.38 million hectares. This rapid increase in oil palm production has led to a significant rise in waste, including oil palm empty fruit bunches (OPEFB). OPEFB waste from the oil palm processing process is produced in a considerable amount, which is around 20–25% of the total weight of the fresh fruit harvested [2].

OPEFB contain approximately 30–40% cellulose and 20–35% lignin, making them a potential source of lignocellulose for further utilization [3]. The high lignin content needs to be reduced through delignification because it can inhibit access to the cellulose fraction. OPEFB cellulose obtained from lignification has superior physical characteristics such as good biocompatibility, high porosity, and large surface area [4]. One of the main drawbacks of cellulose is its insolubility in water, which limits its application and utilization. Modification of cellulose's structure into derivative compounds, such as carboxymethyl cellulose

Applied Science and Engineering Progress, Vol. 19 No. 4, 2026, 8193

(CMC), is one of the strategic efforts to increase the value of cellulose [5].

CMC offers good water solubility, hydrophilic properties, and stability, making it suitable for a wide range of applications. CMC can be produced from a variety of other lignocellulose materials such as rice straw, sawdust, banana peels, and corn stalks [6], [7]. CMC can be further synthesized into gel granules, thereby increasing its functional value and expanding its potential as an environmentally friendly adsorbent for liquid waste treatment [8].

Previous studies have explored the synthesis of alginate-CMC gel granules using various cellulose sources, such as corn stalks [9]. Some studies have successfully utilized other lignocellulose materials, such as rice straw [10], banana stem waste [11], and bagasse [12], as natural raw materials in CMC production for alginate-CMC gel formulations. However, the use of OPEFB as a source of CMC for gel granule synthesis is still rarely researched. OPEFB alginate-CMC gel granules have vast application potential, especially as an adsorbent in the treatment of liquid waste such as methylene blue (MB). MB is a cationic dye commonly used in the textile industry, which can pollute the aquatic environment if not adequately treated [13]. A study showed that alginate-CMC-based gel granules were able to maintain an adsorption efficiency of more than 80% despite repeated use and showed good regeneration resistance [14].

The characteristics of calcium alginate gel granules are generally evaluated based on surface area, pore size, and mechanical properties. Increased mechanical strength and stability of gel granules during synthesis are generally achieved by using crosslinking agents such as calcium chloride ($CaCl_2$) [15]. The use of $CaCl_2$ as a crosslinking agent can improve the three-dimensional structure of gel granules, thereby enhancing their water-absorption capacity and stability under various conditions [16]. The selection of the correct concentration will affect the pore structure and determine the balance between the flexibility and mechanical strength of the gel granules. Efficient absorption can be achieved when gel granules have a well-defined pore structure, a high surface area, and adequate mechanical stability.

Despite the growing development of alginate–CMC-based adsorbents, most previous studies have focused on CMC derived from agricultural residues such as rice straw, banana stems, bagasse, and corn stalks, with limited attention given to OPEFB as a cellulose source. Recent studies have reported the preparation of OPEFB-derived hydrogels crosslinked with $CaCl_2$ [17] and CMC-based systems using alternative crosslinking agents such as $FeCl_3$ [18], demonstrating the feasibility of waste-derived biopolymer materials for environmental applications. Furthermore, recent advancements in waste-derived hydrogels for environmental remediation [19] highlight the increasing interest in developing sustainable adsorbents from localized industrial residues. However, the comparative evaluation of crosslinking concentration effects in OPEFB-based alginate–CMC composite systems remains underexplored. In particular, systematic investigation of $CaCl_2$ concentration and its direct correlation with swelling behavior, surface morphology, and methylene blue adsorption performance has not been comprehensively addressed in OPEFB-derived gel systems.

Therefore, this study provides a focused and systematic evaluation of $CaCl_2$ crosslinking concentrations (3–7%) in alginate–CMC gel beads synthesized from OPEFB-derived CMC. The novelty of this work lies in establishing the relationships among crosslinking density, structural characteristics, and methylene blue adsorption performance within a sustainable, waste-derived biopolymer framework. By optimizing crosslinking conditions to balance mechanical stability, porosity, and adsorption efficiency, this research not only advances the development of environmentally sustainable alginate–CMC-based adsorbents but also promotes the valorization of palm oil industry waste into high-value-added functional materials. The findings provide a scientific basis for determining the optimal crosslinking concentration and support the future development of OPEFB-based materials for wastewater treatment applications.

2 Materials and Methods

2.1 *Materials*

Tools used include analytical balance (Mettler Toledo), Field Emission-Scanning Electron Microscopy (FE-SEM) (Thermo Scientific Quattro S), Fourier Transform Infrared Spectroscopy (FTIR) (Agilent Cary 630), UV-Vis spectrophotometer (Shimadzu UV-1800), oven (Memmert UN 110), vortex (Gemmy VM-300), viscometer (OEM NDJ-8S), magnetic stirrer, porcelain cup, desiccant, burette, bulb, glassware (Iwaki), mesh, spatula, hotplate, iron tweezers, 26G syringe, tripod, clamp, cuvette, and spray bottle.

The materials used include OPEFB cellulose, filter paper, aluminum foil, tissues, aquadest, propanol, 96% w/w and 70% w/w ethanol, 12% w/w and 17.5% w/w NaOH solutions, sodium chloroacetate solids, glacial acetic acid, 65% w/w methanol, universal pH strips, 5% w/v potassium chromate indicators, ferroin indicators, standard 0.1 N silver nitrate solution, a solution of NaCl 0.1 M, 96% w/w H_2SO_4, blue methylene solids, sodium alginate, and $CaCl_2$ were all obtained from Sigma, Merck, and Supelco.

2.2 *Methods*

2.2.1 Synthesis of carboxymethyl cellulose (CMC) [20]

The CMC synthesis process (Figure 1) is carried out by mixing 5 grams of cellulose with a propanol-ethanol solvent mixture, then adding 12% NaOH and stirring at 700 rpm before letting it sit for 1 hour, followed by the addition of sodium chloroacetate dissolved in ethanol and the homogenization process at 55 °C for 3 hours under continuous stirring at 700 rpm, before finally neutralizing the reaction mixture using glacial acetic acid until pH 7 is reached, followed by filtering, washing, and drying. The determination of moisture content is carried out according to SNI 01-3182-1992 by drying the sample in a porcelain cup until a constant weight is obtained. The viscosity value was determined according to SNI 06-6989.11-2004 using the NDJ-8S viscometer after dissolving 4 grams of CMC in 200 mL of distilled water and stirring it for 30 minutes. The purity level of sodium chloride was measured according to SNI 06-6989.19-2004 by dissolving the sample in 65% methanol, depositing for 5 hours, and titrating with 0.1 M silver nitrate solution using a potassium chromate indicator to determine the end point. The particle size of CMC OPEFB was measured using a particle size analyzer to evaluate the size distribution of the synthesized material.

2.2.2 Synthesis of alginate-CMC OPEFB gel granules [21]

One gram of sodium alginate is dissolved in 25 mL of aqueous solution. Furthermore, CMC OPEFB was added with an alginate to CMC ratio of 1:2. The mixed solution is then dripped using a 26G syringe into a $CaCl_2$ solution with concentration variations of 3%, 4%, 5%, 6%, and 7%, as much as 100 mL. This concentration range was selected to ensure sufficient structural integrity while maintaining adequate porosity of the gel network. The distance between the syringe and the solution is 3 cm, and

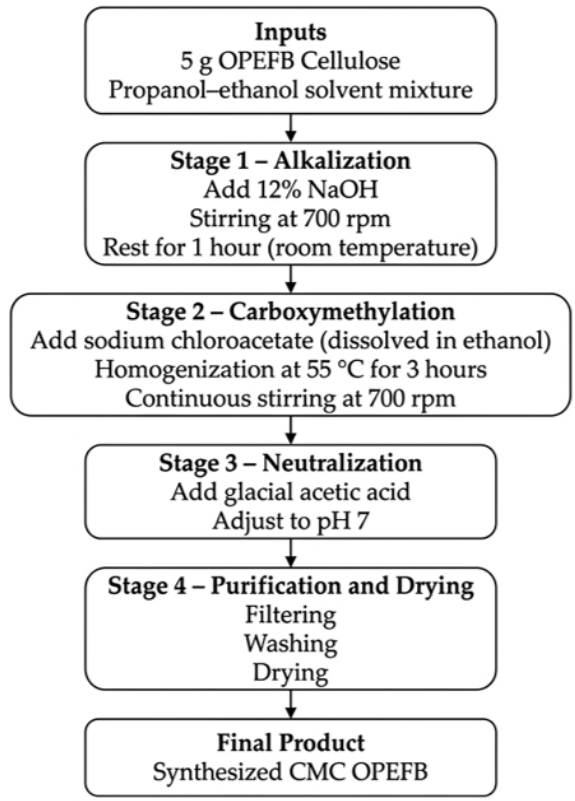

Figure 1. Synthesis of CMC.

then the solution is left to sit for 24 hours. The gel granules formed are then filtered and rinsed using distilled water and then dried using an oven at 37 °C for 24 hours.

2.2.3 Alginant-CMC gel granule swelling test [21]

Alginate beads was prepared by soaking 30 mg of CMC in 10 mL of aqueous solution. Alginate-CMC beads are then weighed after soaking for 8 days and weighed every 24 hours. The swelling ratio was calculated using the following Equation (1):

$$Swelling\ (\%) = \frac{W_e - W_0}{W_0} \times 100\% \quad (1)$$

where W_0 is the initial dry weight of the gel granules (g) and W_e is the weight of the swollen granules (g).

2.2.4 Morphological analysis with scanning electron microscope (SEM)

The sample is placed and mounted on the SEM specimen stand using a double-sided carbon adhesive,

Applied Science and Engineering Progress, Vol. 19 No. 4, 2026, 8193

with the cross-section facing vertically upwards or pointing towards the objective lens. SEM is operated with standard parameters, namely a voltage of 20 kV, a point size of 50, and a working distance of 10 mm. A distance of 10 mm was chosen as a compromise in the signal acquisition setup for optimal X-ray detection and enumeration.

2.2.5 *Analysis of functional clusters with infrared Fourier transform (FTIR)*

Characterization of functional groups was carried out using Fourier Transform Infrared (FTIR) spectroscopy with the Bruker Alpha II instrument. Analysis was performed on CMC–alginate gel granule samples with a wavenumber range of 4000–500 cm^{-1}. The sample was dried first, then finely ground with potassium bromide (KBr) and pressed into transparent pellets using a pressure of 80 kN before being analyzed.

2.2.6 *Adsorption of OPEFB alginate-CMC gel granules against methylene blue*

Testing of the activity of gel granules against methylene blue (MB) dyes was carried out using an MB solution with an initial concentration of 50 ppm. A total of 10 mL of the solution was capped and placed in a test tube according to the variation in $CaCl_2$ concentration. Furthermore, three gel granules of each variation in $CaCl_2$ concentration were put into the MB solution, and their absorbance was measured with a UV-Vis spectrophotometer at a wavelength of 664 nm. Testing of the gel granule activity lasted for 7 days, with monitoring of the decrease in absorbance at each variation in $CaCl_2$ concentration. The adsorption capacity was calculated using the following Equation (2):

$$q_t = \frac{(C_0 - C_e)}{m} \times V \quad (2)$$

Where q_t (mg/g) is the adsorption capacity, C_0 (mg/L) is the initial MB concentration, C_e (mg/L) is the final concentration of MB after adsorption, V (L) is the volume of the solution, and m (g) is the mass of the gel granules.

After the adsorption test is completed, the swelling test is again performed to evaluate the change in the physical properties of the gel granules after absorbing the blue methylene solution. The results of this swelling measurement will be compared with the results of the swelling test before the adsorption process to assess the effect of adsorption on the swelling ability of the gel granules.

3 Result and Discussion

3.1 *Synthesis and characterization of CMC OPEFB*

The processing of OPEFB begins with the enumeration stage to reduce the size of the particles to facilitate the process of separating the constituent fractions (Figure 2). The chopped OPEFB is then isolated with cellulose to purify the fiber components by removing lignin and other extractives. This isolation process is important because OPEFB is a lignocellulose biomass with the main content in the form of cellulose, hemicellulose, and lignin [19], [22].

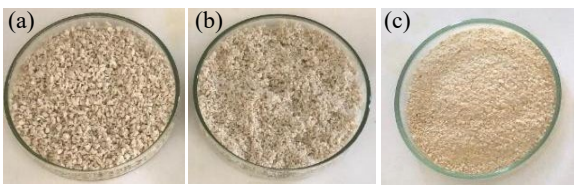

Figure 2. Preparation of samples. (a) OPEFB cellulose before homogenization; (b) OPEFB cellulose after homogenization; (c) CMC OPEFB.

Based on the results of the synthesis that has been carried out, the color of the final product of CMC often shows a yellowish to brownish hue (Figure 1). This discoloration is thought to be related to the heating effect during the synthesis process [23]. This color visualization is one of the important aspects, especially in the application of foodstuffs, because it gives an initial impression for consumers of product quality [24]. In addition to the visual aspect, other parameters, such as moisture content, also need to be analyzed to assess the quality and stability of CMC products as a whole.

The results of cellulose conversion from OPEFB in this study were obtained as much as 2.5 kg of dry cellulose from 30 kg of wet OPEFB raw materials, or equivalent to 8.33% of the yield. This yield shows conversion efficiency that is in line with the characteristics of lignocellulose biomass. Most of the initial mass is lost due to the release of lignins, extractives, and other non-structural components. The yield value is still within a reasonable range for oil palm biomass that has gone through the process of delignification and bleaching [25]. These results

confirm that OPEFB has excellent potential as an alternative source of cellulose to be developed into derivative products of economic value, such as carboxymethyl cellulose (CMC).

OPEFB cellulose has coarse fibers, so it requires a homogenization process to obtain uniform particle sizes so that the modification reaction runs optimally. Good homogenization will increase the surface area and ensure that the cellulose reacts perfectly in the formation of CMC. CMC synthesis takes place through two main stages, namely alkalization and carboxymethylation (Figure 3) [26]. In the alkalinization stage, a 10% NaOH solution together with isopropanol and ethanol helps to open the crystalline structure of cellulose to facilitate the diffusion of sodium chloroacetate at a later stage [27], [28].

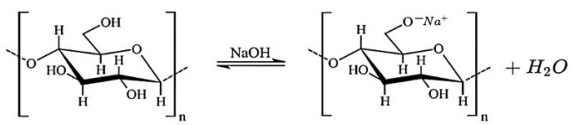

Figure 3. Alkalization [29].

The carboxymethylation process involves a reaction between sodium chloroacetate and the cellulose –OH group in an etherification reaction, forming a carboxymethyl group that increases the solubility and rheological properties of CMC (Figure 4) [30]. Suboptimal reaction conditions can produce by-products such as sodium glycolate [31], so pH and temperature control are critical [32].

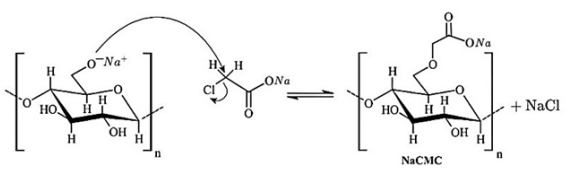

Figure 4. Carboxymethylation [26].

The particle size of CMC OPEFB obtained in this study was 1724 nm. The quality of CMC is assessed from several parameters, one of which is moisture content. This study reported an average moisture content of 11.60%, still within a reasonable range and consistent with previous studies [33]. Factors such as the drying process and the hygroscopic properties of CMC affect moisture content [34], and high moisture content can degrade quality and accelerate degradation [35].

The viscosity of CMC OPEFB was at an average value of 25.20 mPas, according to the general characteristics of CMC based on lignocellulose biomass [36]. This value is influenced by reaction conditions and purity levels [37]. The purity level of CMC to chloride ions reached 93.19%, indicating that the carboxymethylation reaction took place efficiently and the washing process was effective [37]. CMC purity standards are generally above 60% [38], making these results suitable for technical applications, although further improvements are needed for food or pharmaceutical applications [38].

3.2 *Synthesis of alginate-CMC OPEFB gel granules*

The synthesis of OPEFB alginate-CMC gel granules using $CaCl_2$ as a cross-linking agent is the process of ionic gel formation through the interaction between carboxylate groups on the polymer and divalent calcium ions (Ca^{2+}). Sodium alginate, which is soluble in water, will bind Ca^{2+} to form a stable three-dimensional structure [39]. The synthesis of these gel granules uses variations in the concentration of $CaCl_2$ crosslinking agents, namely 3%, 4%, 5%, 6%, and 7%. This concentration range was selected based on previous reports indicating that moderate $CaCl_2$ concentrations are effective in forming stable alginate-based gel networks without inducing excessive structural densification [40], [17]. The variation in $CaCl_2$ concentration was designed to modulate the crosslinking density within the alginate–CMC matrix, as the availability of Ca^{2+} ions directly governs the formation of ionic bridges between carboxylate groups [41]. At low concentrations (<3%), limited Ca^{2+} availability may result in incomplete ionic crosslinking, leading to weak gel matrices with reduced mechanical stability and excessive swelling behavior [42]. In contrast, higher $CaCl_2$ concentrations (>7–8%) promote increased ionic interactions and tighter polymer chain packing, producing a more compact and rigid network structure [40], [43]. Although enhanced crosslinking improves structural integrity, excessive densification may reduce pore accessibility, restrict water uptake, and limit internal diffusion pathways within the gel matrix [44]. Therefore, the selected 3–7% concentration range enables systematic evaluation of the balance between network stability, swelling characteristics, structural openness, and adsorption performance of OPEFB-based alginate–CMC gel granules. The composition of the ingredients in the synthesis of gel granules follows the ratio in the previous study [21], which is with the

proportion of alginate and CMC of 1:2. The addition of CMC from OPEFB to the system also contributes to carboxymethyl groups that are able to interact with calcium ions. The more carboxymethyl groups, the stronger the polymer matrix, and the more it improves the structural stability of the gel granules [8]. This interaction results in a tighter polymer network, which is able to resist deformation and maintain shape under varied environmental conditions [45]. CMC also acts as a viscosity-stabilizing agent, which increases structural resistance during drying processes or repeated discharging [46].

The process of gel granule synthesis is carried out by the dropping method, which involves dripping a polymer solution into a $CaCl_2$ solution to produce dense spherical gel granules (Figure 5). This technique is easy to apply and does not require complex equipment, making it a widely used method on both laboratory and semi-industrial scales [47]. In addition to producing a relatively uniform shape of the gel granules, this method also allows control of the granule size by regulating the viscosity of the solution and the dropper rate [48]. This is important in ensuring the consistency of the physical characteristics and performance of the granules in subsequent applications. The combination of alginate and CMC from OPEFB with the cross-binding agent $CaCl_2$ provides distinct advantages in applications such as encapsulation, controlled release, or absorption of active substances.

$CaCl_2$ was chosen as a cross-linking agent because it is water-soluble, non-toxic, and capable of forming strong cross-bonds with carboxylate groups, making it ideal for active ingredient applications in food, environmental, and pharmaceutical fields. The selection of $CaCl_2$ is also based on its ability to form reversible ionic bonds, which allows the control of the release properties of the active substance from the gel matrix [49]. In addition, the use of $CaCl_2$ in natural polymer systems, such as alginate and CMC, has been shown to improve the thermal stability and mechanical resistance of gel granules, making them resistant to environmental changes [50]. The high calcium content also facilitates the formation of tight, stable three-dimensional networks, which are very important in controlled-discharge systems and adsorption applications [51]. The gel solution that has been dripped into the $CaCl_2$ solution is then left to sit for 24 hours to ensure optimal formation of a cross-bond between the calcium ions and the polymer matrix. Next, the formed gel granules are filtered and dried at 37 ºC for 24 hours to remove moisture and obtain a stable final shape.

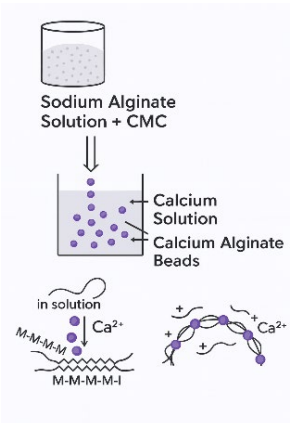

Figure 5. Gel granule synthesis dropping method.

3.3 *Swelling test of alginate-CMC OPEFB gel granules*

The swelling test is one of the important parameters in the characterization of polymer-based gel granules. This test aims to determine the ability of gel granules to absorb water or other solvents that are directly related to the gel tissue structure, porosity, and fluid retention capacity. The swelling rate affects the effectiveness of gel granules in applications such as encapsulation, active-substance release, and adsorption of liquid waste [52].

The swelling test results showed changes in the morphology of the gel granules under dry conditions (Figure 6). Dry gel granules have a small size (0.7 cm) and a relatively hard surface due to the absence of solvent molecules in the polymer tissue. The process of swelling against water causes a significant increase in size due to the entry of water molecules into the gel matrix that forms hydrogen bonds with hydrophilic groups. Swelling of the methylene blue solution results in a larger size (1.7 cm) than water swelling (1.3), as well as a change in color to deep blue, indicating adsorption of the dye. This demonstrates that the pore structure and active groups in the gel play important roles in the material's absorption capacity and changes in its visual properties. The swelling power is also greatly influenced by the concentration of cross-binding agents. The role of $CaCl_2$ as a cross-binding agent will determine the density of the gel tissue. The higher the concentration of Ca^{2+}, the tighter the cross-links between polymer chains, so that the space between the networks narrows and the swelling capacity decreases [53]. This is in accordance with the results obtained in the swelling test of OPEFB alginate-CMC gel granules against water.

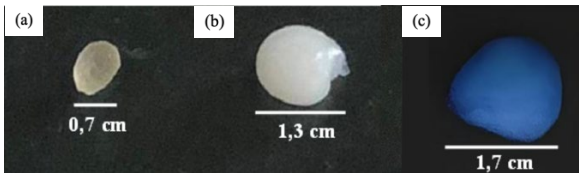

Figure 6. Alginate-CMC OPEFB gel granules. a) dry, b) wet, and c) after absorbing methylene blue.

The swelling test of alginate-CMC gel granules made from OPEFB at various $CaCl_2$ concentrations (3–7%) for 8 days showed a decreasing trend in water absorption over time (Figure 7). At a concentration of $CaCl_2$ 3%, the initial swelling value reached 167.06% on the first day, then decreased sharply to about 9.01% on the 8th day. The increase in $CaCl_2$ concentration was seen to reduce the average swelling power. At 4% $CaCl_2$, the average swelling on the first day was 121.51%; at 5%, 128.63%; at 6%, 137.26%; and at 7%, 153.36%. This pattern shows that higher calcium concentrations strengthen the cross-links between polymer chains, making the gel structure tighter and inhibiting water absorption. A consistent decrease in swelling from the first to the eighth day across all treatments also showed that the gel water's absorption capacity decreased over time, likely due to the release of calcium ions or the relaxation of the polymer structure during immersion.

The results of the swelling test on OPEFB alginate-CMC gel granules can be used to predict the stability and mass-transfer capabilities for applications such as blue methylene adsorption. Optimal swelling allows the dye molecules to diffuse more easily into the pores of the gel granules, thereby improving the adsorption efficiency [54]. The swelling test on methylene blue liquid waste also provides an idea of the extent to which the gel matrix can maintain its integrity in an alkaline dye environment, which is particularly relevant for textile waste treatment applications [55]. The results of the swelling test of OPEFB alginate-CMC gel granules against methylene blue also showed a decrease; namely, the higher the $CaCl_2$ concentration, the lower the swelling power of the gel granules (Figure 8).

The swelling results showed that controlling the $CaCl_2$ concentration is essential for balancing the mechanical properties and absorption capacity of the gel granules. Concentrations that are too high actually make the gel too stiff, thus limiting the diffusion of molecules. Similar results were also reported in previous studies [56], which state that excessive concentrations of cross-binding agents inhibit the

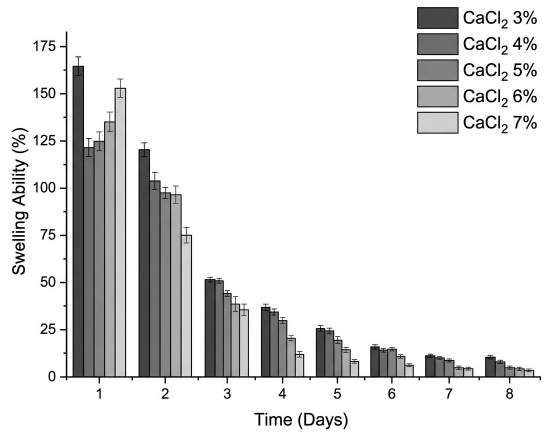

Figure 7. Swelling power decrease of gel granules against water.

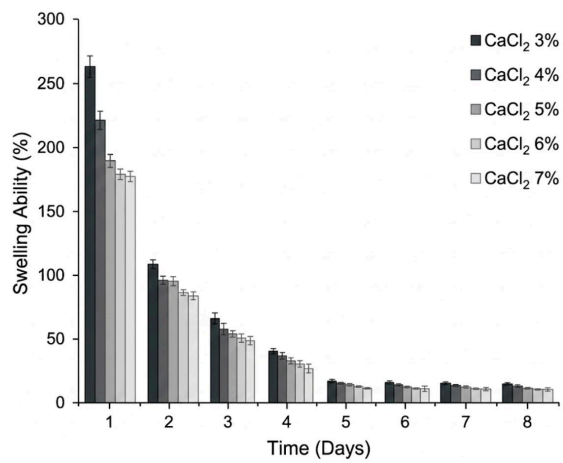

Figure 8. Decreased swelling power of gel granules against blue methylene.

expansion of hydrogel networks due to limited space between polymer chains. A high swelling value at the beginning indicates that the gel granules absorb water quickly. However, after reaching the saturation point or when the gel tissue begins to soften, there is a weakening of the structure that leads to a decrease in the swelling value [57].

Too high a swelling can cause the gel structure to become brittle and easily destroyed, while too low a swelling can limit the diffusion of the active substance into the gel matrix [58]. Therefore, control of synthesis parameters such as the concentration of cross-binding agents is key in obtaining swelling properties that are suitable for the target application. In the context of liquid waste adsorption, a balance

between swelling capacity and mechanical stability is essential to ensure a longer service life as well as the effectiveness of the contaminant [59]. Adjustments to polymer composition and process conditions can also be used to modify the properties of swelling to match the characteristics of the targeted waste [60]. This shows the importance of a design approach based on material properties to produce gel granules with optimal performance.

In addition, swelling characterization can also help understand the mechanism of interaction of water or solvent molecules with polymer matrices. The hydrophilic functional groups in CMC and alginate contribute to the ability of gel granules to form hydrogen bonds with water, increasing the rate of imbibition and solvent distribution in gel tissues [61]. This mechanism is important for the development of drug delivery systems or the encapsulation of active substances that require controlled release. In dye adsorption applications, the porosity exposed by swelling also facilitates the diffusion of the target molecule into the internal adsorption site [62]. Therefore, swelling testing is not only a physical parameter, but also an important indicator in the design and optimization of material functions.

A deep understanding of swelling properties also opens up opportunities to develop biobased gel granules, such as OPEFB, that are sustainable and environmentally friendly. The use of agricultural waste, such as OPEFB, as a source of CMC supports the principle of the circular economy by utilizing abundant, low-value biomass [63]. Further research can be focused on the optimization of carboxymethylation processes, polymer formulations, and cross-linking conditions to produce materials with swelling properties that meet industrial needs.

3.4 *Functional group analysis with FTIR*

FTIR is an important technique for identifying functional groups and changes in chemical structure by measuring a compound's infrared spectrum [64]. This analysis is used to verify chemical modifications and polymer interactions, as well as to compare the purity of materials.

Based on the FTIR spectra of cellulose, synthesized CMC OPEFB, and commercial CMC (Figure 9), cellulose exhibited a characteristic –OH stretching band at 3332 cm^{-1} and a C–H stretching vibration at 2887 cm^{-1}. In commercial CMC, these bands appeared sharper at 3334 cm^{-1} and 2921 cm^{-1}, respectively. Commercial CMC also showed a prominent asymmetrical $–COO^-$

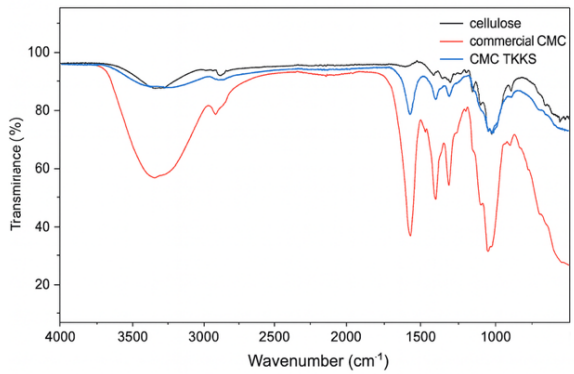

Figure 9. FTIR spectrum of cellulose, CMC OPEFB, and commercial CMC.

stretching band at 1585 cm^{-1}, accompanied by bands at 1413 cm^{-1} and 1323 cm^{-1}, which are typical for carboxymethyl groups and indicate a relatively higher degree of substitution [65].

For the synthesized CMC OPEFB, the –OH band shifted to 3234 cm^{-1}, the C–H band appeared at 2879 cm^{-1}, and the $–COO^-$ band was detected at 1586 cm^{-1}, confirming the successful introduction of carboxymethyl groups during the etherification process (Figure 10). The shift of the –OH band suggests a modification of the hydrogen-bonding network in the cellulose structure [66]. The incorporation of carboxymethyl groups disrupts the ordered intra- and intermolecular hydrogen bonds of native cellulose, reducing crystallinity and promoting a more amorphous polymer structure typical of carboxymethylated cellulose derivatives [67].

FTIR analysis was also used to study structural changes due to cross-bonding with Ca^{2+} (Table 1), where increased intensity and shift of the $–COO^-$ band indicate strong ionic interactions [68]. Bands of 1030–1050 cm^{-1} remain present, indicating that the basic structure of CMC–alginate is preserved. A band shift of 1420–1460 cm^{-1} indicates an increase in carboxylate bond strength, which improves gel stability and thermal resistance as reported by previous studies [69]. Specifically, the asymmetric stretching vibration of $–COO^-$ groups shifted from 1586 cm^{-1} (CMC OPEFB) to lower wavenumbers (1572–1569 cm^{-1}) after gel formation, indicating coordination between Ca^{2+} ions and carboxylate groups. This shift reflects a change in bond environment due to ionic bridge formation, which reduces the vibrational energy of the carboxylate group and confirms the development of a crosslinked network structure [17].

Table 1. Identification of FTIR cellulose, CMC, alginate-CMC gel granules, and $CaCl_2$ influence.

Functional group	Wavenumber (cm^{-1})						
	Cellulose	**CMC Commercial**	**OPEFB CMC**	**BA-CMC 3%**	**BA-CMC 7%**	**$CaCl_2$**	**Based on literatures**
O-H *Stretching* (Hydroxyl)	3332	3334	3234	3312	3278	3259	3200-3400 [72-74]
C-H *Stretching* (Alkanes)	2887	2921	2879	2865	2861	2948	2850-2950 [72- 74]
C=O *Stretching* (Carbonyl)	-	1571	1586	1572	1569	1614	1550-1650 [75], [76]
C-H *Bending*	1426	1413	1407	1437	1435	1425	1400-1450 [72- 74]
C-O *Stretching* (Ester)	1258	1323	1321	-	-	-	1200-1350 [74], [76]
C-O-C *Stretching* (Ether)	1104	1117	1113	1126	1125	1123	1050-1150 [72], [75]
C-H *Bending* (Aromatic)	-	-	-	995	993	973	950-1000 [75], [76]

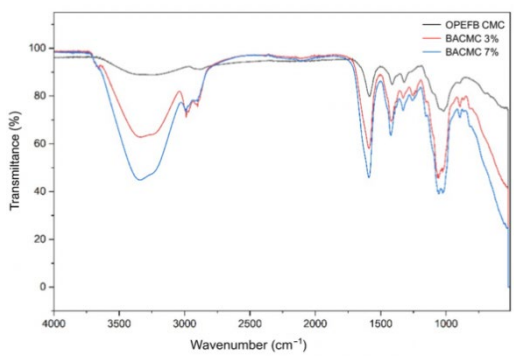

Figure 10. FTIR spectrum of CMC OPEFB and alginate-CMC gel granules at 3% and 7%.

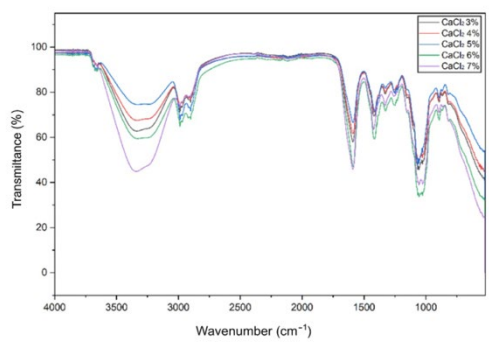

Figure 11. FTIR spectrum influences $CaCl_2$ concentration

Variations in $CaCl_2$ concentrations also affected the intensity of the COO^- bands at 1614 and 1425 cm^{-1} (Figure 11). At concentrations of 6–7%, the bands are more intense and defined, exhibiting stronger ionic interactions. The increased sharpness and intensity of the bands at 1614 and 1425 cm^{-1} at higher $CaCl_2$ concentrations indicate a higher crosslinking density, suggesting that more Ca^{2+} ions participate in ionic bridging between polymer chains. The reduced intensity of the –OH stretching band at 7% further supports restricted chain mobility and decreased hydrogen bonding freedom due to a more compact and rigid network [17]. At a concentration of 7%, a decrease in the intensity of the –OH band signifies a stiffer cross-link. The bands at 1250, 1320 cm^{-1}, and 1056–1057 and 892 cm^{-1} also changed, reflecting an increase in the regularity of polymer tissues [70]. This structural adjustment is important to optimize the physical properties of the gel for encapsulation and release applications of active substances [71].

Overall, the IR spectrum attests to the important influence of $CaCl_2$ concentrations on the chemical structure and cross-linking levels of alginate-CMC granules. Increased carboxylate band intensity at higher $CaCl_2$ concentrations indicates that more Ca^{2+} ionic bridges are formed between polymer chains. This supports the formation of a stiffer gel structure, improving mechanical strength and stability in adsorption applications. This characterization provides important evidence for optimizing the gel granule formulation, as the appropriate cross-linking level affects functional properties such as swelling

power and durability. $CaCl_2$ variation is a key factor in controlling the end-properties of natural polymer-based beads [77].

3.5 *Morphological analysis results by SEM*

Surface morphological analysis using the Scanning Electron Microscope (SEM) is an important characterization technique for understanding the microstructure and physical properties of natural polymer-based gel granules, such as alginate-CMC. SEM analysis showed significant structural differences between CMC and cellulose samples. SEM results for cellulose showed a more orderly morphology with parallel fibril orientation and a dense, smooth surface. These morphological characteristics indicate that cellulose has a high degree of crystallinity, a compact structure, and good mechanical strength, but a lower water absorption capacity.

The results of the SEM analysis of CMC OPEFB (Figure 12) show an irregular surface morphology with layered structures and gaps, indicating more amorphous and open material properties. The existence of these layers indicates that there has been a disruption of the cellulose crystalline structure due to the carboxymethylation process. This modification results in a more porous surface and increases the affinity of CMC to water, further implicating higher swelling capacity and adsorption ability than pure cellulose [78].

These morphological characteristics support the potential of CMC to be applied in the field of dye adsorption, gel formation, and as a matrix in the release system of active substances. There are no noticeable cracks or structural damage to the cellulose surface, indicating high structural stability. This suggests that the carboxymethylation process not only plays a role in the modification of chemical structure but also exerts a significant influence on the physical characteristics and morphology of materials [37].

Through SEM analysis, the geometric shape, size distribution, roughness, cracks, and density of polymer tissues formed by the cross-linking process with Ca^{2+} ions can be observed. These morphological characteristics have a direct effect on mechanical properties, structural stability, and diffusion ability in waste separation and absorption applications. Variations in the concentration of cross-linking agents such as $CaCl_2$ affect the cross-bonds that are formed, thereby causing significant changes in the surface topography of the gel granules [79].

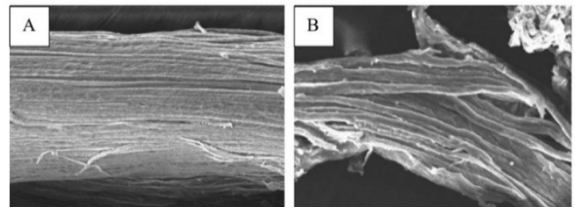

Figure 12. SEM analysis results: a) Cellulose 250x magnification and b) CMC OPEFB 500x magnification.

The results of SEM observation of OPEFB alginate–CMC gel granules before the blue methylene (MB) adsorption process showed a surface morphology that tends to be dense with relatively small pore structures (Figure 13). The surface texture looks uneven, which is characterized by the presence of shallow curves indicating the existence of polymer networks that are strongly bonded together. This structure reflects that the gel-forming process results in a dense polymer matrix so that the ability of the molecules to diffuse into the pores can be limited. According to previous studies [80], the ionic interaction between the carboxyl group of CMC and the cation of alginate plays an important role in forming a compact three-dimensional framework. In addition, low porosity at this early stage can affect the adsorption capacity because the effective surface area is relatively small. A similar study found that alginate-based materials with low CMC ratios tend to form less-exposed surfaces [81]. The morphological conditions before MB adsorption can be used as a reference to evaluate the effectiveness of structural modification in improving adsorption properties. These characteristics confirm the importance of regulating polymer composition and gelation conditions to obtain optimal morphology. The morphology of alginate–CMC gel granules after MB adsorption showed significant changes to the surface. The results of SEM analysis showed the appearance of microcracks and loss of regularity in the surface structure, indicating a strong interaction between MB molecules and polymer matrices. This condition is consistent with previous research, which found that dye molecules can stick to the pore walls as they fill the internal cavity, thereby reducing effective porosity [82]. This condition is also evident in other studies on alginate-CMC-based films, which show that dye adsorption modifies the surface texture [83].

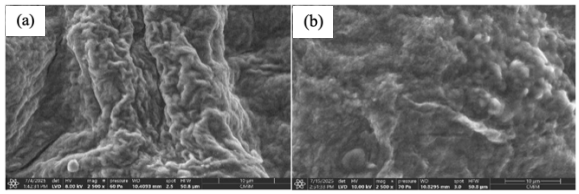

Figure 13. SEM analysis results of Alginate-CMC OPEFB Gel Granules (a) before absorbing MB and (b) after absorbing MB, 2500X magnification.

The formation of microcracks and nodular layers also shows the deposition of MB molecules on the surface as well as in the pores, indicating that the adsorbate–adsorbent interaction is not only physical, but also involves chemical interactions, especially electrostatic bonds between negatively charged groups (carboxylate groups) and MB [84]. This change suggests that the adsorption process can widen the structural gap and that some of the active area is actually covered by bound molecules, so that further adsorption ability may decrease in subsequent cycles [85].

3.6 *Adsorption capacity results for blue methylene*

Adsorption capacity is an important parameter in determining the performance of a material in the solute separation process, especially in the treatment of liquid waste containing coloured organic compounds such as methylene blue. The value of adsorption capacity reflects the amount of substances that can be held by the mass unit of the adsorbent, so that it is directly related to the efficiency and effectiveness of the utilization of the material. Evaluation of this capacity is generally carried out through the measurement of the residual solute concentration after the contact process has taken place, which is then calculated based on the mass of the adsorbent used.

The results of the blue methylene adsorption capacity test showed an increase in adsorption capacity as the initial MB concentration increased for all variations in $CaCl_2$ concentration (Figure 14). These results show that the higher the $CaCl_2$ concentration, the lower the adsorption capacity. The optimum condition was obtained at a $CaCl_2$ concentration of 3% (>3 mg/g), whereas at 6–7% it reached only 0.5–1.1 mg/g. This indicates the influence of anionic forces, i.e., Ca^{2+} ions compete with MB molecules to bind to the adsorbent surface, thus limiting the number of active sites available to MB [86].

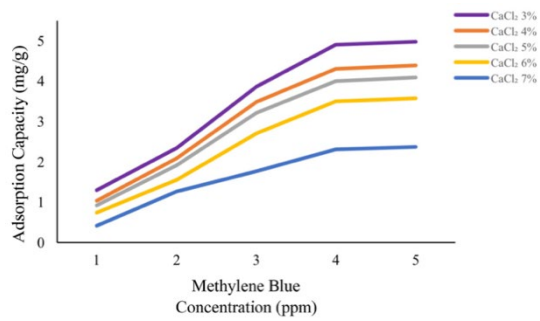

Figure 14. Adsorption capacity against blue methylene.

The difference in adsorption capacity between treatments is evident at higher initial MB concentrations (Figure 14). Treatment with 3% $CaCl_2$ showed the greatest improvement compared to other treatments, so it can be considered the most effective. The results of this graph support the understanding that the wider the surface and the more active groups available, the better the adsorption ability. This condition confirms that the presence of low amounts of Ca^{2+} ions does not overclose access to the active site. Thus, the adsorption performance is more optimal when the modification is carried out at a moderate level.

Furthermore, the adsorption capacity is closely related to the swelling behavior of the hydrogel. Lower $CaCl_2$ concentrations produce a lower degree of ionic crosslinking, allowing the CMC matrix to swell more extensively in aqueous media [17]. The expansion of the polymer network generates larger internal pores and diffusion pathways, facilitating the penetration of water and dissolved MB molecules into the hydrogel structure and enabling greater access to internal carboxylate ($–COO^-$) active sites [17]. In contrast, higher $CaCl_2$ concentrations (6–7%) result in a more densely crosslinked and compact network that restricts polymer chain mobility and limits swelling capacity [87]. The reduced swelling constrains internal pore accessibility, thereby hindering MB diffusion into the hydrogel matrix and ultimately decreasing the overall adsorption capacity [87]. This trend is consistent with the swelling results discussed previously, where gels prepared with lower $CaCl_2$ concentrations exhibited higher swelling ratios.

At higher concentrations of $CaCl_2$, the gel structure becomes tighter as strong cross-links are formed. This condition makes the gel granules sturdier but also reduces porosity and the number of active sites that MB molecules can occupy [88]. In contrast,

lower $CaCl_2$ results in a looser gel structure with open pores, making it easier for MB molecules to enter the adsorbent despite reduced mechanical strength [89]. These results show a balance between mechanical properties and absorption efficiency. If the cross-bond is too tight, the absorbency is reduced; On the other hand, if it is too loose, the structure is easily damaged, but absorption is better.

In addition to the influence of $CaCl_2$, the properties of the adsorbent surface, such as surface area, pore size, and functional group, also greatly determine the adsorption capacity. Recent research suggests that chemical or physical changes to the adsorbent surface can strengthen adsorbent-dye interactions, resulting in a significant increase in adsorption capacity [90]. This can be done through chemical activation, the addition of reinforcing agents, or thermal treatments to improve the pore structure. With the proper modification strategy, the adsorbent can have a balanced combination of mechanical strength and adsorption efficiency.

4 Conclusions

Based on the results of this study, alginate–CMC OPEFB gel granules were successfully synthesized using varying $CaCl_2$ concentrations, which significantly influenced their physicochemical and morphological properties. Increasing $CaCl_2$ concentration produced a denser gel network that restricted polymer chain mobility. The optimum performance was achieved at 3% $CaCl_2$, which exhibited the highest methylene blue adsorption capacity (3.5991 mg/g) and the maximum swelling ratio (65.35%). FTIR analysis confirmed the formation of ionic crosslinking between carboxylate groups and Ca^{2+} ions, indicated by characteristic bands around 1614 cm^{-1}, while SEM observations showed that changes in pore morphology affected diffusion and adsorption behavior.

Future studies should focus on optimizing the alginate–CMC formulation to balance swelling capacity, mechanical stability, and adsorption efficiency. Additional investigations under real wastewater conditions, exploration of alternative crosslinking agents, and evaluation of regeneration performance are necessary to improve material stability and reusability. Furthermore, assessment of production costs and scalability will be essential to support the potential industrial application of OPEFB-based adsorbents as sustainable materials for wastewater treatment.

Acknowledgment

Author would like to thank to all parties who have provided support in completing this research, especially to the Plantation Fund Management Agency (BPDP) for funding this research with the number PRJ -146/DPKS/2024, to the analyst and research technicians involved who have provided guidance, direction, and valuable input during the research process, and laboratory colleagues who have assisted in the implementation of experiments and data analysis.

Author Contributions

F.D.: conceptualization, investigation, writing and reviewing; T.P.: investigation, methodology, writing an original draft; Y.F.: research design, data analysis, data curation; F.A.E.: investigation, data curation, writing—reviewing and editing, project administration; D.N.K. and I.P.S.: investigation, data curation, data analysis; D.H.G.: conceptualization, methodology; P.R.: investigation, methodology, reviewing. All authors have read and agreed to the published version of the manuscript.

Conflicts of Interest

The authors declare no conflict of interest.

Declaration of generative AI and AI-assisted technologies in the writing process

The authors utilized the ChatGPT tool to enhance the language and readability of the manuscript.

References

[1] Oil Palm Plantation Fund Management Agency, "Development of Palm Oil Plantation Human Resources as an Effort Toward Sustainable Indonesian Palm Oil," *Annual Report 2021*, 2021.

[2] E. Shabrina , R. Alfarizki, N Hidayat, N. Sunyoto , S. Suhartini, and I. Nurika, "Effect of nutrient supplementation on biological pretreatment of *Paenibacillus* sp. for delignification of oil palm empty fruit bunches," *Jurnal Teknologi Pertanian*, vol. 26, no. 2, pp. 123–134, 2025, doi: 10.21776/ub.jtp.2025.026.02.3.

[3] F. Dimawarnita, U. Perwitasari, S. Marsudi, Y. Faramitha, and S. Suharyanto, "The utilization of

oil palm empty fruit bunches for growth of oyster mushroom (*Pleurotus ostreatus*) and biodelignification process during planting cycle, " *Agrivitas: Journal of Agricultural Science*, vol. 44, no. 1, pp. 165–177, 2023, doi:10.17503/agrivita.v44i1.2311.

[4] T. Aziz, A. Farid, and F. Haq, "A review on the modification of cellulose and its applications," *Polymers*, vol. 14, no. 15, p. 3206, 2022. doi: https://doi.org/10.3390/polym14153206

[5] M. Karataş, B. Erzen, and E. Aydoğmuş, "Carboxymethyl cellulose: Synthesis, properties, and applications," *Academic Research and Reviews in Engineering Sciences*, Platanus Publishing, 2023, doi:10.5281/zenodo.1006077.

[6] S. Tantavoranart, W. Raongjant, V. Khum-In, and K. Saricheewin, "Agricultural waste valorization: Field application of rice straw-derived carboxymethyl cellulose for irrigation water reuse," *Environmental Technology*, vol. 47, no. 3, pp. 431–448, 2025, doi: 10.1080/09593330.2025.2585216.

[7] J. Kumla *et al.* "Cultivation of mushrooms and their lignocellulolytic enzyme production through the utilization of agro-industrial waste," *Molecules*, vol. 25, no. 12, p2811, 2020, doi: 10.3390/molecules25122811.

[8] A. Devina, R. Maryana, M. Fahri, A. K. H. Hasibuan, and T. Agustianto, "Optimization of carboxymethyl cellulose (CMC) synthesis in production of hydrogel from *Ananas comosus L.* leaves," *Journal Sains Student Research*, vol. 3, no. 6, pp. 433–446, 2025, doi:10.61722/jssr.v3i6.6479.

[9] L. N. Khusna, E. Yulianti, L. M. Khoiroh, and V. N. Istighfarini, "Synthesis and characterization of beads alginate carboxymethyl cellulose from corn stalk (*Zea mays*) using $BaCl_2$ as crosslink with variation concentration," in *Advances in Social Science, Education and Humanities Research*, vol. 529, 2021, doi:10.2991/assehr.k.210421.055.

[10] P. Rodsamran and R. Sothornvit, "Rice stubble as a new biopolymer source to produce carboxymethyl cellulose-blended films," *Carbohydrate Polymers*, vol. 171, no. 1, pp. 94–101, 2017. doi: https://doi.org/10.1016/j.carbpol.2017.05.003

[11] A. F. Aminuddin and N. H. Baharim, "Removal of methylene blue in aqueous solution by using bioadsorbent from banana pseudo stem," *ASEAN Journal of Life Sciences*, vol. 1, no. 2, pp. 46–50, 2021.

[12] M. Dwiyaniti, A. E. Barruna, R. M. Naufal, I. Subiyanto, R. Setiabudy, and C. Hudaya, "Extremely high surface area of activated carbon originated from sugarcane bagasse," *IOP Conference Series: Materials Science and Engineering*, vol. 909, no. 1, Art. no. 012022, 2020, doi: 10.1088/1757-899X/909/1/012022.

[13] C. Vyas and M. Choudhary, "Degradation of methylene blue dye as wastewater pollutant by atmospheric pressure plasma: A comparative study," *arXiv*, 2023, doi: 10.48550/arxiv.2301.11053.

[14] D. Allouss, Y. Essamlali, O. Amadine, A. Chakir, and M. Zahouily, "Response surface methodology for optimization of methylene blue adsorption onto carboxymethyl cellulose-based hydrogel beads: adsorption kinetics, isotherm, thermodynamics and reusability studies," *RSC Advances*, vol. 9, no. 65, pp. 37858–37869, 2019. doi: https://doi.org/10.1039/C9RA06450H

[15] H. Malektaj, A. D. Drozdov, and J. deClaville Christiansen, "Mechanical properties of alginate hydrogels cross-linked with multivalent cations," *Polymers*, vol. 15, no. 14, 2023. doi: https://doi.org/10.3390/polym15143012

[16] P. R. Sari, Dianursanti, and K. C. H. Alifia, "Application of *Spirulina platensis* with cross-linker $CaCl_2$ for making hard capsule shell," *AIP Conference Proceedings*, vol. 2235, Art. no. 020009, 2020, doi:10.1063/5.0002807.

[17] N. F. A. T. Mohamood, A. H. A. Halim, and N. Zainuddin, "Carboxymethyl cellulose hydrogel from biomass waste of oil palm empty fruit bunch using calcium chloride as crosslinking agent," *Polymers*, vol. 13, no. 23, 2021, doi: 10.3390/polym13234056.

[18] S. W. To, R. H. A. Al-Ashwal, N. A. Latif, and M. H. Sani, "Synthesis and characterisation of biodegradable carboxymethyl cellulose microcarriers from oil palm empty fruit bunch for therapeutic applications," *Cellulose*, vol. 32, no. 1, pp. 483–503, 2024, doi: 10.1007/s10570-024-06269-x.

[19] A. A. Sulianto *et al.,* (2025). "Pectin-based hydrogels produced from banana and mango peels as a potential approach to removing heavy metal ions from contaminated water," *Repository of TBU Publications (Univerzita Tomase Bati ve Zlín)*. [Online]. Available: http://publikace.k.utb.cz/handle/10563/1012751

[20] F. Dimawarnita, and T. Panji, "Synthesis of carboxymethyl cellulose from ex-baglog of oyster mushroom (*Pleurotus ostreatus*)," *E-Journal Menara Perkebunan*, vol. 86, no. 2, 2018, doi:10.22302/iribb.jur.mp.v86i2.304.

[21] M. Jannah Munawwaroh and Miftahul, "Sintesis dan karakterisasi beads alginat–karboksimetil selulosa dari batang jagung menggunakan variasi $CaCl_2$," Thesis, Universitas Islam Negeri Maulana Malik Ibrahim Malang, Indonesia, 2019.

[22] F. Dimawarnita, U. Perwitasari, S. Marsudi, Y. Faramitha, and Suharyanto, "The utilization of oil palm empty fruit bunches for growth of oyster mushroom (*Pleurotus ostreatus*) and biodelignification process during planting cycle," *Agrivitas: Journal of Agricultural Science*, vol. 44, no. 1, pp. 165–177, 2023, doi:10.17503/agrivita.v44i1.2311.

[23] A. Wijayani, K. Ummah, and S. Tjahjani, "Characterization of carboxy methyl cellulose (CMC) from *Eichhornia crassipes* (Mart.) Solms," *Indonesian Journal of Chemistry*, vol. 5, no. 3, pp. 228–231, 2005, doi:10.22146/ijc.21795.

[24] H. S. Wahyuni, S. Yuliasmi, H. S. Aisyah, and D. Riati, "Characterization of synthesized sodium carboxymethyl cellulose with variation of solvent mixture and alkali concentration," *Macedonian Journal of Medical Sciences*, vol. 7, no. 22, pp. 3878–3881, 2019, doi: 10.3889/oamjms.2019.524.

[25] S. Mulyati, E. Sriwahyuni, P. Wulandari, and R. Rahmawati, "Extraction and characterization of cellulose from oil palm empty fruit bunches," *IOP Conference Series: Earth and Environmental Science*, vol. 482, no. 1, Art. no. 012006, 2020, doi: 10.1088/1755-1315/482/1/012006.

[26] R. Jalil, M. Sarif, P. Elham, and S. Hashim, "Synthesis of carboxymethyl cellulose (CMC) from delignified *Dyera costulata*," *Malaysian Journal of Chemical Engineering and Technology*, vol. 5, no. 2, pp. 110–116, 2022, doi: 10.24191/mjcet.v5i2.19773.

[27] A. Koistinen, H. Wang, E. Hiltunen, T. Vuorinen, and T. Maloney, "Refinability of mercerized softwood kraft pulp," *Cellulose*, vol. 31, no. 10, pp. 6471–6484, 2024, doi: 10.1007/s10570-024-05999-2.

[28] F. Dimawarnita, T. Panji, and Y. Faramitha, "Peningkatan kemurnian selulosa dan karboksimetil selulosa (CMC) hasil konversi limbah TKKS melalui perlakuan NaOH 12%," *E-Journal Menara Perkebunan*, vol. 87, no. 2, 2019, doi:10.22302/iribb.jur.mp.v87i2.339.

[29] M. Yáñez-S., B. Matsuhiro, S. Maldonado, R. González, J. Luengo, and O. Uyarte, "Carboxymethylcellulose from bleached organosolv fibers of *Eucalyptus nitens*: synthesis and physicochemical characterization," *Cellulose*, vol. 25, no. 5, pp. 2901–2914, 2018, doi: 10.1007/s10570-018-1766-7.

[30] F. Wahid, L. Huang, X. Zhao, W. Li, Y. Wang, S. Jia, and C. Zhong, "Bacterial cellulose and its potential for biomedical applications," *Biotechnology Advances*, vol. 53, Art. no. 107856, 2021, doi:10.1016/j.biotechadv.2021.107856.

[31] V. Pushpamalar, S. Langford, M. Ahmad, and Y. Lim, "Optimization of reaction conditions for preparing carboxymethyl cellulose from sago waste," *Carbohydrate Polymers*, vol. 64, no. 2, pp. 312–318, 2006, doi: 10.1016/j.carbpol.2005.12.003.

[32] B. Panda, S. Patnaik, D. Purohit, and A. Dubey, "Impact of sodium starch glycolate on physico-chemical characteristics of mouth dissolving film of fexofenadine," *NeuroQuantology*, vol. 20, no. 6, pp. 3183–3192, 2022, doi: 10.14704/nq.2022.20.6.NQ22759.

[33] M. C. da Silva Farias et al., "Thermal degradation of carboxymethyl cellulose (CMC) in saline solution for applications in petroleum industry fluids," *Polymers*, vol. 17, no. 15, Art. no. 2085, 2025, doi: 10.3390/polym17152085.

[34] R. D. Múnera-Tangarife, E. Solarte-Rodríguez, C. Vélez-Pasos, and C. I. Ochoa-Martínez, "Factors affecting the time and process of CMC drying using refractance window or conductive hydro-drying," *Gels*, vol. 7, no. 4, Art. no. 257, 2021, doi: 10.3390/gels7040257.

[35] E. Pinto et al., "Cellulose processing from biomass and its derivatization into carboxymethylcellulose: A review," *Scientific African*, vol. 15, Art. no. e01078, 2021, doi: 10.1016/j.sciaf.2021.e01078.

[36] D. Silsia, Z. Efendi, and F. Timotius, "Characterization of carboxymethyl cellulose (CMC) from palm midrib," *Jurnal Agroindustri*, vol. 8, no. 1, pp. 53–61, 2018, doi: 10.31186/j.agroind.8.1.53-61.

[37] S. Rashid and H. Dutta, "Physicochemical characterization of carboxymethyl cellulose

from differently sized rice husks and application as cake additive," *LWT - Food Science and Technology*, vol. 154, Art. no. 112630, 2021, doi: 10.1016/j.lwt.2021.112630.

[38] S. Hidayat, Susanty, N. Riveli, B. J. Suroto, and I. Rahayu, "Synthesis and characterization of CMC from water hyacinth for lithium-ion battery applications," *AIP Conference Proceedings*, vol. 1927, no. 1, Art. no. 030023, 2018, doi: 10.1063/1.5021216.

[39] W. Wang et al., "Sodium alginate modifications: A critical review of current strategies and emerging applications," *Foods*, vol. 14, no. 22, Art. no. 3931, 2025, doi: 10.3390/foods 14223931.

[40] J. Fu, J. X. Yap, C. P. Leo, and C. K. Chang, "Carboxymethyl cellulose/sodium alginate beads incorporated with calcium carbonate nanoparticles and bentonite for phosphate recovery," *International Journal of Biological Macromolecules*, vol. 234, Art. no. 123642, 2023, doi: 10.1016/j.ijbiomac.2023.123642.

[41] H. Nasution et al., "Hydrogel and effects of crosslinking agent on cellulose-based hydrogels: A review," *Gels*, vol. 8, no. 9, Art. no. 568, 2022, doi: 10.3390/gels8090568.

[42] M. A. da Silva, A. C. K. Bierhalz, and T. G. Kieckbusch, "Alginate and pectin composite films crosslinked with Ca^{2+} ions: Effect of the plasticizer concentration," *Carbohydrate Polymers*, vol. 77, no. 4, pp. 736–742, 2009, doi: 10.1016/j.carbpol.2009.02.014.

[43] J. Li, Y. Wu, J. He, and Y. Huang, "A new insight to the effect of calcium concentration on gelation process and physical properties of alginate films," *Journal of Materials Science*, vol. 51, no. 12, pp. 5791–5801, 2016, doi: 10.1007/s10853-016-9880-0.

[44] Y. Samchenko, K. Terpilowski, K. Samchenko, L. Golovkova, O. Oranska, and O. Goncharuk, "Calcium alginate/laponite nanocomposite hydrogels: Synthesis, swelling, and sorption properties," *Coatings*, vol. 14, no. 12, Art. no. 1519, 2024, doi: 10.3390/coatings14121519.

[45] J. Brydson, "States of aggregation in polymers," in *Plastics Materials*, 7th ed. Elsevier, 1999, ch. 3, pp. 43–58, doi: 10.1016/B978-075064132-6/50044-9.

[46] A. Hashem, S. Farag, and S. Badawy, "Carboxymethyl cellulose: Past innovations, present applications, and future horizons," *Results in Chemistry*, vol. 17, Art. no. 102534, 2025, doi: 10.1016/j.rechem.2025.102534.

[47] M. D. Khan, A. Singh, M. Z. Khan, S. Tabraiz, and J. Sheikh, "Current perspectives, recent advancements, and efficiencies of various dye-containing wastewater treatment technologies," *Journal of Water Process Engineering*, vol. 53, Art. no. 103579, 2023, doi: 10.1016/j.jwpe. 2023.103579.

[48] B. Sapra, S. Parveen, A. K. Tiwari, and O. Silakari, "Design strategies for smart hydrogels: From concept to application," in *Hydrogels - Smart Materials for Biomedical Applications*, IntechOpen, 2024, doi: 10.5772/intechopen. 1006716.

[49] J. Shu, D. J. McClements, S. Luo, C. Liu, and J. Ye, "Advances of biopolymer-based emulsion gels: Fabrication, design, and application," *Trends in Food Science & Technology*, vol. 165, Art. no. 105335, 2025, doi: 10.1016/j.tifs.2025. 105335.

[50] Z. Feyissa, G. D. Edossa, N. K. Gupta, and D. Negera, "Development of double crosslinked sodium alginate/chitosan based hydrogels for controlled release of metronidazole and its antibacterial activity," *Heliyon*, vol. 9, no. 9, Art. no. e20144, 2023, doi: 10.1016/j.heliyon.2023. e20144.

[51] X. Zhang, K. Wang, J. Hu, Y. Zhang, Y. Dai, and F. Xia, "Role of a high calcium ion content in extending the properties of alginate dual-crosslinked hydrogels," *Journal of Materials Chemistry A*, vol. 8, no. 47, pp. 25390–25401, 2020, doi: 10.1039/D0TA09315G.

[52] M. M. H. Rumon, "Advances in cellulose-based hydrogels: Tunable swelling dynamics and their versatile real-time applications," *RSC Advances*, vol. 15, no. 15, pp. 11688–11729, 2025, doi: 10.1039/D5RA00521C.

[53] C. Qiao and X. Cao, "Swelling behavior of physically cross-linked gelatin gels in varied salt solutions," *Journal of Macromolecular Science, Part B*, vol. 53, no. 10, pp. 1609–1620, 2013, doi: 10.1080/00222348.2013.837302.

[54] G. R. Deen, Y. L. Tan, M. R. Yalini, C. H. Mah, and T. W. Teo, "Synthesis, swelling characteristics, and dye adsorption mechanism of a new stimuli-responsive cationic hydrogel," *European Journal of Advanced Chemistry Research*, vol. 3, no. 1, pp. 12–24, 2022, doi: 10.24018/ejchem.2022.3.1.86.

[55] Y. Zeng, X. Tang, Y. Qin, A. Maimaiti, X. Zhou, and Y. Guo, "Enhanced removal of methylene blue from wastewater by alginate/carboxymethyl cellulose–melamine sponge composite," *International Journal of Biological Macromolecules*, vol. 244, Art. no. 125280, 2023, doi: 10.1016/j.ijbiomac.2023.125280.

[56] K. Salma-Ancane, A. Sceglovs, E. Tracuma, J. K. Wychowaniec, K. Aunina, and A. Ramata-Stunda, "Effect of crosslinking strategy on the biological, antibacterial and physicochemical performance of hyaluronic acid and ε-polylysine based hydrogels," *International Journal of Biological Macromolecules*, vol. 208, pp. 995–1008, 2022, doi: 10.1016/j.ijbiomac.2022.03.207.

[57] R. H. Pritchard and E. M. Terentjev, "Swelling and de-swelling of gels under external elastic deformation," *Polymer*, vol. 54, no. 26, pp. 6954–6960, 2013, doi:10.1016/j.polymer.2013.11.006.

[58] S. Argin, P. Kofinas, and Y. M. Lo, "The cell release kinetics and the swelling behavior of physically crosslinked xanthan–chitosan hydrogels in simulated gastrointestinal conditions," *Food Hydrocolloids*, vol. 40, pp. 138–144, 2014, doi:10.1016/j.foodhyd.2014.02.018.

[59] S. Satyam and S. Patra, "Innovations and challenges in adsorption-based wastewater remediation: A comprehensive review," *Heliyon*, vol. 10, no. 9, Art. no. 29573, 2024, doi: 10.1016/j.heliyon.2024.e29573.

[60] M. García-Morales, P. Partal, F. Navarro, and C. Gallegos, "Effect of waste polymer addition on the rheology of modified bitumen," *Fuel*, vol. 85, no. 7–8, pp. 936–943, 2005, doi: 10.1016/j.fuel.2005.09.015.

[61] I. Sathisaran and M. Balasubramanian, "Physical characterization of chitosan/gelatin–alginate composite beads for controlled release of urea," *Heliyon*, vol. 6, no. 11, Art. no. e05495, 2020, doi: 10.1016/j.heliyon.2020.e05495.

[62] Z. Hu et al., "Adsorption characteristics of bacterial cellulose membranes toward methylene blue dye in aqueous environment," *Gels*, vol. 11, no. 9, Art. no. 721, 2025, doi: 10.3390/gels11090721.

[63] M. R. Almafie, I. Royani, and I. Sriyanti, "Synthesis of microcrystalline cellulose from oil palm empty fruit bunches through sequential chemical processing," *Results in Engineering*, vol. 29, Art. no. 109091, 2026, doi: 10.1016/j.rineng.2026.109091.

[64] A. N. V. L. Kavya, S. Sundarrajan, and S. Ramakrishna, "Identification and characterization of micro-plastics in the marine environment: A mini review," *Marine Pollution Bulletin*, vol. 160, Art. no. 111704, 2020, doi: 10.1016/j.marpolbul.2020.111704.

[65] M. Y. Eliza, M. Shahruddin, J. Noormaziah, and W. D. W. Rosli, "Carboxymethyl cellulose (CMC) from oil palm empty fruit bunch (OPEFB) in the new solvent dimethyl sulfoxide (DMSO)/tetrabutylammonium fluoride (TBAF)," *Journal of Physics: Conference Series*, vol. 622, no. 1, Art. no. 012026, 2015, doi: 10.1088/1742-6596/622/1/012026.

[66] I. Moussa, R. Khiari, A. Moussa, M. N. Belgacem, and M. F. Mhenni, "Preparation and characterization of carboxymethyl cellulose with a high degree of substitution from agricultural wastes," *Fibers and Polymers*, vol. 20, no. 5, pp. 933–943, 2019, doi: 10.1007/s12221-019-8665-x.

[67] . Dimawarnita, Y. Faramitha, H. T. Prakoso, I. Puspitasari, D. N. Kalbuadi, and D. Prasetyo, "Characterization of cellulose from oil palm empty fruit bunches by fast delignification process with different solvents," *E-Journal Menara Perkebunan*, vol. 91, no. 2, pp. 71–84, 2023, doi: 10.22302/iribb.jur.mp.v91i2.542.

[68] S. K. Papageorgiou, E. P. Kouvelos, E. P. Favvas, A. A. Sapalidis, G. E. Romanos, and F. K. Katsaros, "Metal–carboxylate interactions in metal–alginate complexes studied with FTIR spectroscopy," *Carbohydrate Research*, vol. 345, no. 4, pp. 469–473, 2009, doi: 10.1016/j.carres.2009.12.010.

[69] T. K. V. Urquiza, O. P. Pérez, and M. G. Saldaña, "Effect of the cross-linking with calcium ions on the structural and thermo-mechanical properties of alginate films," *MRS Proceedings*, vol. 1355, Art. no. 1355-ii04-03, 2011, doi: 10.1557/opl.2011.1136.

[70] T. Anirudhan, C. V. Sekhar, and S. S. Nair, "Polyelectrolyte complexes of carboxymethyl chitosan/alginate based drug carrier for targeted and controlled release of dual drug," *Journal of Drug Delivery Science and Technology*, vol. 51, pp. 569–582, 2019, doi: 10.1016/j.jddst.2019.03.036.

[71] T. Yang, L. Cao, J. Song, and A. G. Skirtach, "Tuning nanostructure of gels: From structural

and functional controls to food applications," *Gels*, vol. 11, no. 8, Art. no. 620, 2025, doi: 10.3390/gels11080620.

[72] S. K. Padmanabhan, L. Lamanna, M. Friuli, A. Sannino, C. Demitri, and A. Licciulli, "Carboxymethylcellulose-based hydrogel obtained from bacterial cellulose," *Molecules*, vol. 28, no. 2, Art. no. 829, 2023, doi: 10.3390/molecules28020829.

[73] W.-X. Yu, Z.-W. Wang, C.-Y. Hu, and L. Wang, "Properties of low methoxyl pectin–carboxymethyl cellulose based on montmorillonite nanocomposite films," *International Journal of Food Science and Technology*, vol. 49, no. 12, pp. 2592–2601, Dec. 2014, doi: 10.1111/ijfs.12590.

[74] D. Wu, J. Guo, M. Sun, and Y. Zhang, "Infrared and terahertz spectra of Pu'er white tea with different degrees of oxidation," *Journal of Food Processing and Preservation*, vol. 2023, Art. no. 3290917, pp. 1–9, 2023, doi: 10.1155/2023/3290917.

[75] B. Gieroba, G. Kalisz, M. Krysa, M. Khalavka, and A. Przekora, "Application of vibrational spectroscopic techniques in the study of natural polysaccharides and their cross-linking process," *International Journal of Molecular Sciences*, vol. 24, no. 3, Art. no. 2630, 2023, doi: 10.3390/ijms24032630.

[76] F. L. Bernard et al., "Development of inexpensive cellulose-based sorbents for carbon dioxide," *Brazilian Journal of Chemical Engineering*, vol. 36, no. 1, pp. 511–521, 2019, doi: 10.1590/0104-6632.20190361s20170182.

[77] M. Tavakol, E. Vasheghani-Farahani, and S. Hashemi-Najafabadi, "The effect of polymer and $CaCl_2$ concentrations on the sulfasalazine release from alginate-N,O-carboxymethyl chitosan beads," *Progress in Biomaterials*, vol. 2, no. 1, Art. no. 10, 2013, doi: 10.1186/2194-0517-2-10.

[78] X. He et al., "Comparison of cellulose derivatives for Ca^{2+} and Zn^{2+} adsorption: Binding behavior and *in vivo* bioavailability," *Carbohydrate Polymers*, vol. 294, Art. no. 119837, 2022, doi: 10.1016/j.carbpol.2022.119837.

[79] Amiruddin, M. A. S. Rijal, and D. M. Hariyadi, "Effect of $CaCl_2$ crosslinker concentration on the characteristics, release and stability of ciprofloxacin HCl–alginate–carrageenan microspheres," *Jurnal Farmasi dan Ilmu Kefarmasian Indonesia*, vol. 10, no. 3, pp. 312–323, 2023, doi: 10.20473/jfiki.v10i32023.312-323.

[80] C. Hu, W. Lu, A. Mata, K. Nishinari, and Y. Fang, "Ions-induced gelation of alginate: Mechanisms and applications," *International Journal of Biological Macromolecules*, vol. 177, pp. 578–588, 2021, doi: 10.1016/j.ijbiomac.2021.02.086.

[81] S. Morozkina et al., "The fabrication of alginate–carboxymethyl cellulose-based composites and drug release profiles," *Polymers*, vol. 14, no. 17, Art. no. 3604, 2022, doi: 10.3390/polym14173604.

[82] F. Liu, Z. Guo, H. Ling, Z. Huang, and D. Tang, "Effect of pore structure on the adsorption of aqueous dyes to ordered mesoporous carbons," *Microporous and Mesoporous Materials*, vol. 227, pp. 104–111, 2016, doi: 10.1016/j.micromeso.2016.02.051.

[83] T. Wang, W. Wang, C. Hu, J. Zheng, Z. Zhu, and B. Liu, "Design of carboxymethyl cellulose/alginate aerogels with anti-fouling and light-driven self-cleaning for enhanced oily wastewater remediation," *Carbohydrate Polymers*, vol. 342, Art. no. 122358, 2024, doi: 10.1016/j.carbpol.2024.122358.

[84] Y. F. Carhuarupay-Molleda, N. M. C. Barboza, S. Pastor-Mina, C. E. D. Valcarcel, Y. G. Palomino-Malpartida, and R. L. Redolfo, "A study of methylene blue adsorption by a synergistic adsorbent alga (*Nostoc sphaericum*)," *Polymers*, vol. 17, no. 15, Art. no. 2134, 2025, doi: 10.3390/polym17152134.

[85] H. Zheng et al., "Recent advances of interphases in carbon fiber-reinforced polymer composites: A review," *Composites Part B: Engineering*, vol. 233, Art. no. 109639, 2022, doi: 10.1016/j.compositesb.2022.109639.

[86] Y. Bakhtaoui, M. B. Ali, M. Ouakki, O. E. Khattabi, N. E. Azzouzi, and B. Srhir, "Efficient adsorption of methylene blue onto raw olive pomace from Moroccan industrial oil mills: Linear and nonlinear isotherm and kinetic modeling with error analysis," *Next Materials*, vol. 9, Art. no. 101072, 2025, doi: 10.1016/j.nxmate.2025.101072.

[87] R. Rakhmetullayeva, B. Khavilkhairat, A. Toktabayeva, N. Mukhamadiyev, E. Nurgaziyeva, and M. Abutalip, "Biopolymer-based hydrogel formulations for improved seed coating performance," *Scientific Reports*, vol.

16, no. 1, Art. no. 1106, 2025, doi: 10.1038/s41598-025-30594-1.

[88] P. Sriamornsak and R. A. Kennedy, "Swelling and diffusion studies of calcium polysaccharide gels intended for film coating," *International Journal of Pharmaceutics*, vol. 358, no. 1–2, pp. 205–213, 2008, doi: 10.1016/j.ijpharm.2008.03.009.

[89] A. W. Putra, H. Hermawan, S. Setyaningrum, and T. Paramitha, "The methylene blue adsorption by calcium alginate–activated carbon composite in fixed bed column," *Fluida*, vol. 17, no. 2, pp. 65–70, 2024, doi: 10.35313/fluida.v17i2.4926.

[90] A. F. M. Streit et al., "New study of the adsorption mechanism of different dye molecules by high porous sludge activated carbon produced from a dairy-treatment effluent plant," *Journal of Environmental Chemical Engineering*, vol. 12, no. 5, Art. no. 113745, 2024, doi: 10.1016/j.jece.2024.113745